Journal of
Synchrotron Radiation

ISSN 0909-0495

Received 8 June 2004
Accepted 22 October 2004

Polychromatic X-ray microdiffraction studies of mesoscale structure and dynamics

G. E. Ice,* B. C. Larson, W. Yang, J. D. Budai, J. Z. Tischler, J. W. L. Pang, R. I. Barabash and W. Liu

Oak Ridge National Laboratory, Oak Ridge, TN 37831-6118, USA. E-mail: icege@ornl.gov

Polychromatic X-ray microdiffraction is an emerging tool for studying mesoscale structure and dynamics. Crystalline phase, orientation (texture), elastic and plastic strain can be nondestructively mapped in three dimensions with good spatial and angular resolution. Local crystallographic orientation can be determined to $\sim 0.01^\circ$ and elastic strain tensor elements can be measured with a resolution of $\sim 10^{-4}$ or better. Complete strain tensor information can be obtained by augmenting polychromatic microdiffraction with a monochromatic measurement of one Laue-reflection energy. With differential-aperture depth profiling, volumes tens to hundreds of micrometers below the surface are accessible so that three-dimensional distributions of crystalline morphology including grain boundaries, triple points, second phases and inclusions can all be mapped. Volume elements below 0.25 μm^3 are routinely resolved so that the grain boundary structure of most materials can be characterized. Here the theory, instrumentation and application of polychromatic microdiffraction are described.

Keywords: strain; deformation; grain growth; grain boundary type.

1. Introduction

The study of materials begins with three questions: (i) What is the elemental composition? (ii) How are the atoms arranged structurally? (iii) What are the defects? Intense synchrotron X-rays beams are particularly powerful probes for answering these questions: X-rays are nondestructive, penetrating and sensitive to both chemical composition and structure. Although millimeter-scale X-ray beams have been extensively applied to study materials, the availability of intense synchrotron beams has stimulated the development of microfluorescence capabilities at synchrotron sources around the world (Sparks, 1980; Chevallier & Dhez, 1997; Langevelde *et al.*, 1990). More recently, there has been a sudden rise in the number of synchrotron microdiffraction experiments aimed at studying local structure (Rebonato *et al.*, 1989; Chung & Ice, 1999; Ice & Larson, 2000; Offerman *et al.*, 2002; Budai *et al.*, 2003; Choi *et al.*, 2003). Indeed, X-ray microdiffraction has emerged as an essential tool for nondestructive characterization of local structure within polycrystalline materials where nearly homogeneous subgrain volumes with mesoscopic length scales of $\sim$0.1–100 μm are heterogeneously distributed. Even with almost perfect single-crystal materials, structural inhomogeneities arising from polycrystalline surface layers, ion-deposited induced strained regions or other inhomogeneities introduced by diffusion, thermal mismatch or mechanical deformation are well suited for analysis by X-ray microdiffraction.

Here we describe the application of polychromatic X-ray microdiffraction to the study of mesoscale structure and dynamics in materials. Although monochromatic methods [*e.g.* three-dimensional X-ray diffraction (Poulsen *et al.*, 2001; Poulsen, 2003)] have advantages for some samples, as described below, polychromatic methods combined with differential aperture X-ray microscopy (DAXM) (Larson *et al.*, 2002) provides a powerful almost universal approach for studying the local structure of materials. Indeed, polychromatic microdiffraction can be used to determine the local phase of crystalline materials, the local orientation and therefore the grain and phase boundary structure, and the local defect distribution including elastic and plastic strain, point and defect clusters. The ability to determine the local elastic strain tensor is particularly important, as strain is a key driving force in mesoscale structural dynamics.

In order to exploit the unique advantages of polychromatic microdiffraction, research groups at the Oak Ridge National Laboratory have worked with colleagues at Howard University, the University of Illinois at Urbana Champaign and the Advanced Photon Source to develop polychromatic microdiffraction at the Advanced Photon Source, Argonne, USA. A parallel two-dimensional polychromatic effort is underway at the Advanced Light Source (Tamura *et al.*, 2003; Valek *et al.*,

2002), with another two-dimensional effort at the Pohang synchrotron in Korea (Lee *et al.*, 2001). Other polychromatic microdiffraction facilities are planned for the Australian and Canadian light sources.

The primary advantage of polychromatic microdiffraction is the ability to determine crystalline structure without sample rotations (Chung & Ice, 1999). This is essential for submicrometer or micrometer spatial resolution diffraction measurements as micrometer-scale volumes move into and out of the beam during sample rotations. As illustrated in Fig. 1, a polychromatic microbeam produces a Laue pattern from each subgrain volume that it illuminates. The overlapping patterns are detected by a CCD detector and are decoded by a differential aperture depth profiling technique (Larson *et al.*, 2002). In the differential aperture technique a highly absorbing wire is translated in small steps near the sample surface. The difference between images collected before and after a small move arises from rays that pass near the leading or trailing edge of the wire. By making a series of these difference measurements across the diffracted Laue pattern and by applying triangulation, the overlapping Laue patterns generated within each subgrain volume along the microbeam can be reconstructed.

In its current configuration, a 50 µm-diameter Pt wire is used as the differential aperture (or knife-edge absorption profiler) to depth resolve the Bragg diffracted intensity from the sample (see Fig. 1). Computer reassembly of the differential intensity distribution for each depth segment along the microbeam is accomplished by collating the differential intensities in each CCD pixel for each step of the profiler. The source of the intensity is then determined by triangulating from the pixel position of the intensity in the CCD to the wire position, and is extrapolated to the beam intersect to determine the source of intensity along the microbeam. This makes it possible to reconstruct full diffraction patterns for submicrometer voxels along the penetration direction. The pixel positions, the geometrical parallax associated with the 20 µm × 20 µm pixel size, the profiler step size, the profiler direction and the circular shape of the Pt wire are all taken into account in the depth analysis.

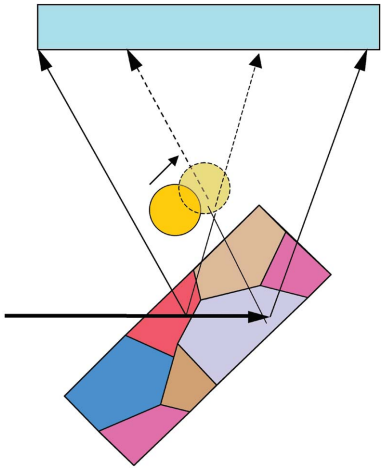

Figure 1
As the polychromatic X-ray beam penetrates the sample, it creates a Laue image from each subgrain it intercepts. The overlapping Laue images are recorded by an X-ray-sensitive CCD. As a wire passes near the sample, it intercepts rays from the sample. The difference between images before and after a small (differential) move are due to rays that pass either near the leading or trailing edge of the wire. By triangulation, the origins of the rays are determined on a pixel-by-pixel basis.

Once the Laue patterns are reconstructed, the local phase, crystal orientation (microtexture), elastic and plastic deformation tensors can all be determined. In principle, four Laue reflections are required to determine the deviatoric strain tensor (Chung & Ice, 1999). The deviatoric strain tensor quantifies the distortion of the unit-cell shape. Reflections in addition to the essential first four are used to improve uncertainty in the deviatoric strain tensor elements. The energy of at least one reflection must be measured to determine the hydrostatic (dilatational) strain (Chung & Ice, 1999).

Polychromatic X-ray microdiffraction is also sensitive to plastic deformation. The introduction of deformation-induced curvature in previously undistorted single crystals is the result of complex dislocation distributions. The dislocation distributions required to accommodate the local lattice curvature generated by plastic deformation processes are referred to as geometrically necessary dislocations (GNDs). The capability to determine local lattice orientations with submicrometer point-to-point spatial resolution provides direct information on the local lattice curvature in three dimensions. This information in turn provides a quantitative measurement of GND densities in plastically deformed regions with the $\sim$1 µm spatial resolution of the curvature measurement.

According to Nye (1953), the dislocation tensor, α_{ij}, can be determined uniquely using the local lattice curvature, which is obtained by three-dimensional measurements of the gradient of local orientation tensor, g_{jl}, through the relation

$$\alpha_{ij} = e_{ikl} g_{jl,k}. \quad (1)$$

e_{ikl} is the permutation tensor and the comma denotes the derivative with respect to the following index. A procedure for quantitatively calculating GND densities considering the possible dislocation slip systems in the structure studied has been discussed by Arsenlis & Park (1999) using a simplex minimization method.

In order to realise the full potential of polychromatic microdiffraction, special instrumentation and software were installed and tested on beamline 7-ID at the APS. The components for a two-dimensional microprobe were retained at 7-ID and three-dimensional operations were moved to the dedicated station 34-ID-E at the Advanced Photon Source. The specialized instrumentation and software are described below.

2. Instrumentation and software for two-dimensional and three-dimensional polychromatic microdiffraction

The key instrumental elements of a polychromatic microprobe are illustrated in Fig. 2. Microbeam performance is typically proportional to source brilliance, and polychromatic microdiffraction performance is specifically proportional to the

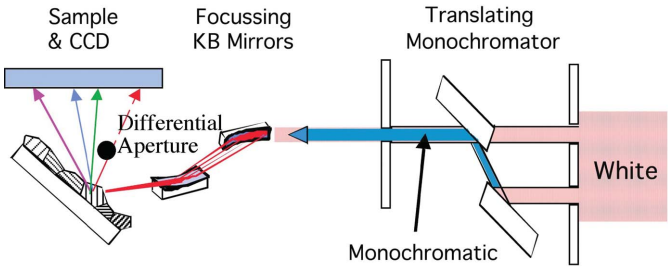

Figure 2
Schematic of the key elements of a three-dimensional polychromatic X-ray microprobe. The intense white-beam source can either be passed directly to the focusing mirrors or monochromated by a special translating monochromator. The KB mirrors focus the polychromatic radiation to a submicrometer spot. The sample is translated with a precision three-axis stage, and a heavy-Z wire runs near the sample surface to decode the origin of the Laue patterns along the incident X-ray beam. The X-ray Laue patterns are detected with an X-ray-sensitive CCD.

integrated source brilliance over a wide bandpass. On ID-7 and ID-34 the source is an APS type A undulator (Xu *et al.*, 1992) with four orders of magnitude greater peak brilliance than bend-magnet sources and about two orders of magnitude greater integrated brilliance between 10 and 20 keV. Typically the undulator spectrum is viewed slightly off axis to broaden the harmonic peaks.

A second key element is a special Si_{111} two-crystal monochromator that can be rapidly inserted into the beam (Ice, Chung, Lowe *et al.*, 2000). The monochromator uses flex pivot rotations to reduce slip and stiction. The monochromator displaces the X-ray beam by about 1 mm but is designed to take the beam to be monochromated from a lower portion of the incident beam so the monochromatic and polychromatic X-ray beams pass through the same exit slit. Although the monochromatic and polychromatic beams exit the same slit, the vertical displacement of the monochromatic beam results in a small angular change of about 20 µrad which displaces the beam focus by ∼2 µm vertically. This displacement is corrected by heating the second crystal so that the d spacing is slightly larger than that of the first crystal. This tilts the monochromatic beam so that the monochromatic beam is parallel and coincident to the polychromatic beam.

A nondispersive total-external-reflecting Kirkpatrick–Baez (KB) focusing system is another key element of the polychromatic microprobe. The elliptical mirrors are made by differentially depositing Au onto superpolished Si substrates with cylindrical curvatures (Ice, Chung, Tischler *et al.*, 2000; Liu, Conley *et al.*, 2003; Liu, Assoufid *et al.*, 2003). The mirrors pass X-rays below ∼22 keV with high efficiency and focus all X-ray wavelengths to a submicrometer spot. Focused beams as small as 300 nm × 400 nm have been measured, and focused beams of ∼500 nm are routinely used.

Samples are mounted on kinematic plates that can be viewed with a microscope prior to experiments and quickly positioned to expose desired sample features to X-ray microdiffraction. Samples are positioned by a computer-controlled three-axis translation stage with optical encoders and a bi-directional reproducibility of ∼50 nm. Directly above the sample a CCD area detector measures the Laue patterns generated by subgrain volumes of the sample exposed to the X-ray beam. The 50 µm-diameter differential aperture wire is driven parallel to and a few hundred micrometers above the sample surface. Because the wire is much closer to the sample than to the detector, the overlapping Laue patterns can be deconvoluted pixel-by-pixel with submicrometer resolution. Special software has been developed that collate the intensity within each pixel to its point of origin along the incident microbeam as a function of wire position. The differential intensities generated when the wire intercepts a Laue spot are used to reconstruct each of the Laue spots from each subgrain volume element. As discussed above, nonlinearities in the CCD, the angular orientation of the CCD, the circular cross section of the profiler wire, and pixel-size-induced parallax are calibrated using a perfect Si crystal and taken into account in the analysis.

Typical micro-Laue patterns are shown in Fig. 3. The key step after resolving the subgrain Laue patterns is to index the patterns (Chung & Ice, 1999; Park *et al.*, 1997; Ravelli *et al.*, 1996; Sheremetyev *et al.*, 1991; Wenk *et al.*, 1997). Indexing is automated by carefully comparing the pattern of angular differences between reflections. The differences are compared with possible indices until a match is found (Chung & Ice, 1999). The precise angles between indexed reflections also determines the elastic strain while changes in the local crystallographic orientation within a single grain are indicative of deformation or elastic strain. As shown in Fig. 4, depth-integrated Laue images often show streaking. Maps of the local crystallographic orientation can be used to determine the local plastic deformation tensor.

The ability to resolve the elastic strain tensor even within single crystals has been demonstrated in an elegant proof-of-principle measurement (Fig. 5*a*) (Larson *et al.*, 2002). Here the deviatoric elastic strain tensor distribution was mapped within an elastically bent perfect single crystal of Si. As shown in Fig. 5(*b*) the deviatoric strain tensor in a flat (*i.e.* unbent) Si plate is zero within the measurement uncertainties. For the elastically bent Si plate, the diagonal deviatoric strain tensor elements change linearly as a function of depth within the bent crystal thickness; the full strain tensor values were obtained

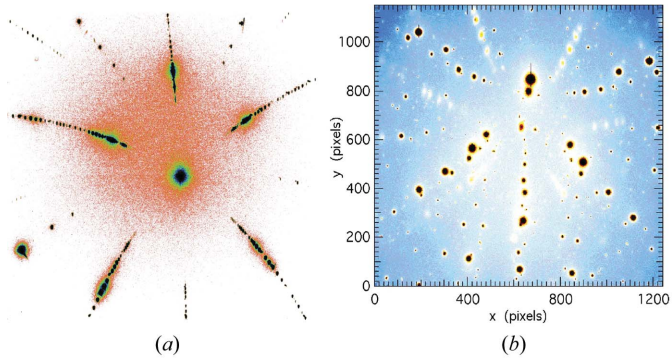

(*a*) (*b*)

Figure 3
Laue patterns from (*a*) GaN film on SiC substrate and (*b*) high-T_c superconductor film and buffer layer on Ni grain.

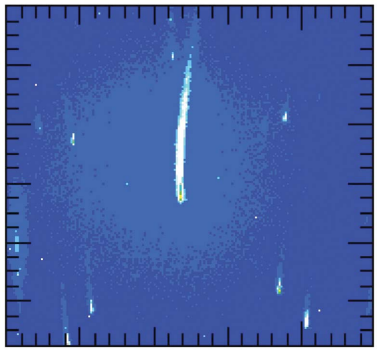

Figure 4
Laue image showing streaking owing to rotations of Cu single-crystal unit cells along the X-ray path. The observed deformation was introduced by a nanoindent.

indirectly (Larson *et al.*, 2002) using measurements showing that anticlastic bending was negligible for the 25 μm-thick plate. Direct measurements of the dilatational strain as a function of depth in an elastically bent Si plate have been made using monochromatic DAXM. Subtle variations in the strain as a function of position in x and y are associated with the complex nature of anticlastic bending near the edges of a plate with finite width (Yang *et al.*, 2003).

3. New scientific directions with the three-dimensional polychromatic microscope

The unprecedented ability to measure local crystalline phase, orientation (texture), elastic and deformation tensors, has enabled new scientific directions with the potential to revolutionize our understanding of mesoscale dynamics and structure. Measurements are already underway to study the dislocation and strain networks near nanoindented regions of Cu single crystals. These measurements provide direct tests of extensive modeling efforts designed to understand the response of materials to nanoindention. Similarly, measurements of the local elastic and plastic response of grain-boundary networks are underway to guide and test multiscale models of polycrystalline materials behavior. We present below some simple examples that illustrate emerging research opportunities made possible by polychromatic microdiffraction.

3.1. Orientation and strain mapping in films

Although this article emphasizes the capabilities of three-dimensional polychromatic X-ray microdiffraction, two-dimensional measurements obtained without differential aperture scanning are useful for many structural studies, particularly when investigating thin-film materials. Used in two-dimensional scanning mode, polychromatic X-ray microdiffraction is ideally suited for providing spatial maps of crystal structure, grain orientations and local strain in deposited layers used in a wide variety of technologies. Recent examples include coated superconductors, ferroelectric actuators and interconnects in integrated circuits (Budai *et al.*, 2003; Tamura *et al.*, 2003; Rogan *et al.*, 2003). Since X-rays

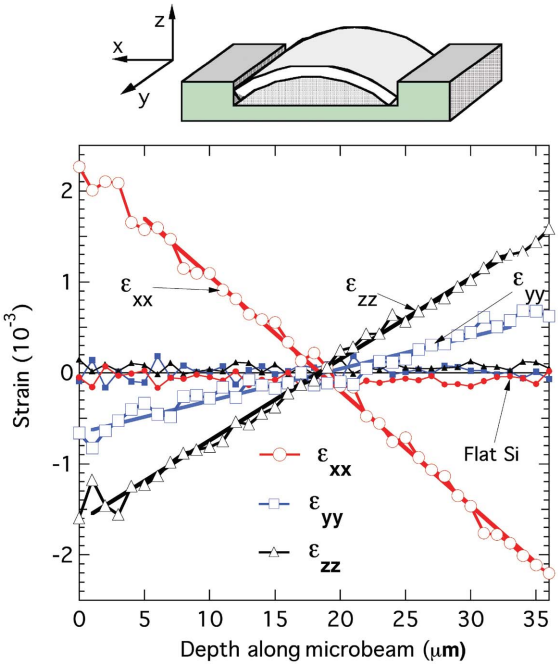

Figure 5
The deviatoric strain tensor in a cylindrically bent single-crystal plate of Si (R = 6.8 mm) can be estimated from the radius of curvature and the position within the thickness of the crystal. Even within a single crystal, the strain tensor elements can be quantitatively measured through the volume. Although the overall elastic behavior of the bent Si can be estimated from simple plate theory, close to edges the Si is actually a beam and exhibits more complex elastic bending behavior.

generally penetrate through thin deposition layers, Laue diffraction patterns from each film layer as well as from the substrate can be mapped simultaneously. In addition, since X-ray measurements are nondestructive and can be carried out in various environments, structural changes such as film delamination (Goudeau *et al.*, 2003) or plastic deformation (Valek *et al.*, 2003) can be monitored during or after materials processing.

Investigations of the epitaxic growth of oxide films deposited on highly textured metal substrates illustrate the two-dimensional scanning capabilities available using polychromatic X-ray microdiffraction (Budai *et al.*, 2003). The motivation for these studies is to understand and control the texture and hence conductivity in superconducting films (Norton *et al.*, 1996). It is known that high-angle grain boundaries in polycrystalline superconductors such as YBaCuO act as weak links, depressing current transport by orders of magnitude. Pulsed laser deposition (PLD) of epitaxic oxide buffer layers and superconducting films on roll-textured Ni foils solves this problem by creating a highly aligned multilayer architecture known as rolling-assisted biaxially textured substrates (RABiTS) (Norton *et al.*, 1996). As shown in Fig. 3(*b*), a typical microdiffraction image from a RABiTs sample consists of the superposition of (001) Laue patterns from the Ni substrate grain, the CeO_2/YSZ oxide buffer layer and the YBCO oxide film. This image reveals an important general feature of RABiTS samples; the (001) Laue patterns for the oxide films are not exactly aligned with the

underlying Ni substrate. Instead, the films exhibit a crystallographic tilt with the (001) planes typically rotating towards alignment with the sample surface.

In order to understand the crystallographic tilting and to exploit it for texture enhancement, a systematic grain-by-grain study of heteroepitaxial tilting was carried out for CeO_2 buffer layers deposited on Ni substrates (mosaic $\sim 8^\circ$ FWHM) (Budai *et al.*, 2003). Fig. 6 shows color-coded orientation maps from both a Ni substrate and a CeO_2 buffer layer in a PLD RABiTS sample. Quantitative analysis of microdiffraction from samples grown at different substrate temperatures revealed two different growth modes: ledge growth and significant lattice tilts at elevated substrate temperatures, and island growth with no tilts at lower temperatures. Further, the magnitude of the local crystallographic tilting was shown to depend linearly on the surface misorientation of the underlying Ni grain. These observations lead to the development of a general geometrical model describing the epitaxic growth of brittle films on ductile substrates. The observed lattice tilts are of practical importance in superconducting applications since they decrease the misorientation between neighboring grains. By maximizing the tilts, the percolation paths for current transport through low-angle grain boundaries can be enhanced.

3.2. Coincident site lattices

An emerging application of the three-dimensional polychromatic microscope is in the study of grain boundaries in polycrystalline materials. Grain boundaries are typically described in terms of the coincident-site-lattice theory (Bollmann, 1982). This theory postulates that grain boundaries are energetically favorable when the lattice sites from one grain overlap with those of the neighbor grain (Fig. 7). The ratio of total lattice sites to the coincident lattice sites is the so called Σ number; more coincidence sites means a smaller Σ number and small-angle grain boundaries have a Σ of almost unity. Only certain integer Σ values are geometrically possible for particular crystal structures (*e.g.* face-centered cubic, tetragonal *etc.*).

Although coincident-site-lattice (CSL) theory is based on a simple geometrical model, extensions include accommodation for dislocations at the grain boundaries (Bollmann, 1982). Furthermore, compelling experimental evidence exists that coincident boundaries have special properties (Watanabe, 1984). Motivated by the need to understand grain boundaries, an active community has developed based on the use of high-resolution electron backscattering diffraction to measure grain orientation, to measure grain boundaries at the surface and hence to infer grain-boundary type (Randle, 1993; Schwartz *et al.*, 2000; Humphreys, 2001). Based on the extensive research from this community, much is known about the statistical distribution of grain boundary types and how grain boundary distributions can be biased by processing (Palumbo & Aust, 1992). This has led to attempts to tailor grain boundary distributions for beneficial physical properties (Palumbo & Aust, 1992) and has stimulated the development of innovative techniques that can destructively characterize grain boundaries in three dimensions (Randle & Davies, 2002).

The three-dimensional polychromatic microscope can build on this body of work by virtue of its exquisite angular resolution and by virtue of its ability to nondestructively map grain boundaries in three dimensions. With the three-dimensional polychromatic X-ray microscope the local orientation of a grain can be measured with $\sim 0.01^\circ$ resolution and with $\sim 0.25\ \mu m^3$ three-dimensional spatial resolution. This allows the grain boundary surface to be characterized both at and below the sample surface. If the grain boundary is not highly curved, then three grain boundary intercepts determine the local grain boundary surface normal (Fig. 8). Because the three-dimensional polychromatic X-ray microscope can measure grain orientation with about two orders of magnitude greater sensitivity than electron backscattering diffraction (EBSD) and because the surface normal can be nondestructively determined, there are key elements of CSL theory that can now be tested for the first time. For example, there are theoretical reasons to suspect that, compared with high Σ boundaries, low Σ boundaries can support more dislocations and hence a greater deviation from their ideal misorientation angle. EBSD measurements are not quite accurate enough to test this hypothesis.

Another question that can now be tested for the first time concerns the nature of grain boundary normals. Whereas EBSD measurements determine the grain-boundary intercepts at the sample surface, X-ray measurements can nondestructively determine the local grain boundary normal deep within the sample. According to CSL theory, a CSL not only has a misorientation but also a favorable normal direction. However, CSLs can possibly accommodate alternative normals by faceting. By measuring the statistical distribution of grain boundary normals and curvatures, the importance of faceting can be characterized. Grain boundary normals and misorientations are particularly interesting in triple junctions where three grains come together and can simultaneously satisfy CSLs between the three grain pairs.

3.3. Sn whiskers

In addition to studies of general mesoscale materials behavior, the three-dimensional polychromatic microscope can provide unique insights into specific materials systems where strain, texture or deformation play an important role in the materials properties. Studies of ultrasonic, fusion and spot welds are underway, as are studies of ion-deposited polycrystalline materials, thermal barrier coatings and electronic materials.

Characterization of whiskers that evolve from Sn films is an application with both practical significance and fundamental importance to mesoscale dynamics; whisker growth is a form of anomalous grain growth where certain grains grow preferentially out of the film. Whisker growth has important implications for the electronics industry, which is trying to eliminate Pb-based solders. Differential grain growth leading to whiskers has been ascribed to inhomogeneous residual stress,

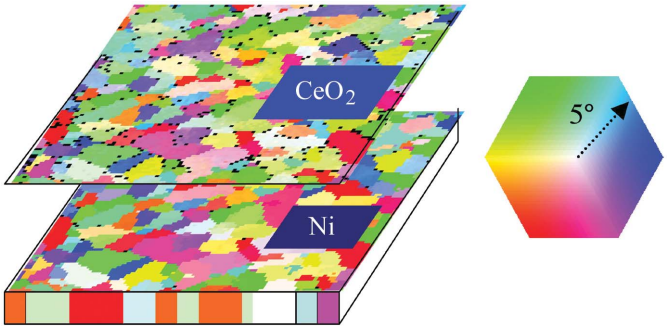

Figure 6
Orientation maps for substrate (Ni) and oxide film (CeO_2) produced by X-ray microdiffraction. Color indicates the angle and direction of [001] with respect to surface normal (white).

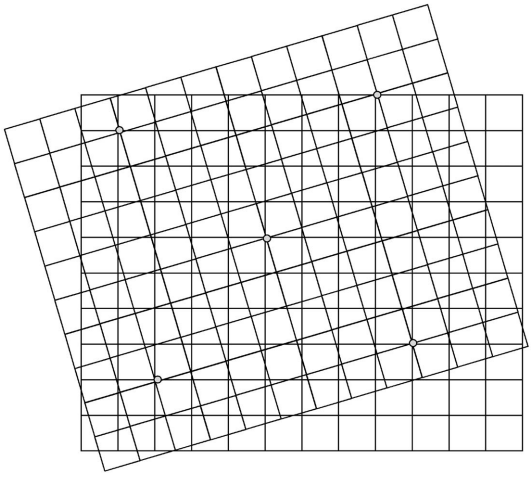

Figure 7
Schematic representation of two lattices with overlapping lattice sites. The coincident sites are widely spaced for this misorientation (high Σ).

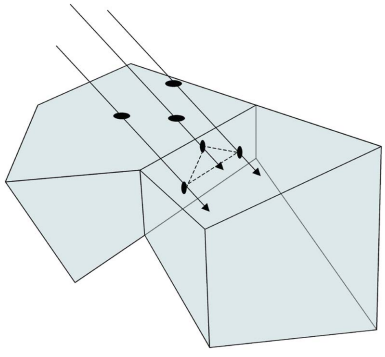

Figure 8
The local grain boundary normal can be determined from three or more grain-boundary intercepts.

special grain orientations, unusual grain boundaries or some combination of all these and other mechanisms (Lee & Lee, 1998). Work underway at the ALS using a two-dimensional polychromatic X-ray microprobe has measured whisker orientation and nearby average strain (Choi *et al.*, 2003). With three-dimensional characterization, a more complete picture of the whisker and its local environment is possible. Essential to test the various hypotheses is the ability to study local strain

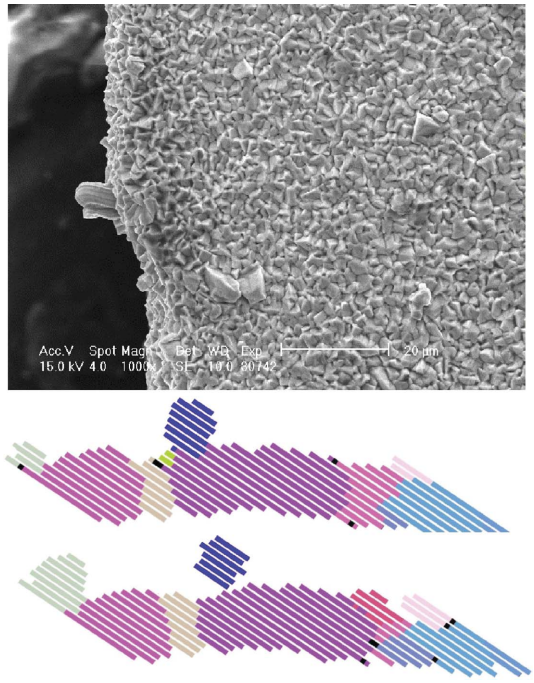

Figure 9
The upper SEM image shows whiskers on a Sn film. The middle and lower false-color images show grain structure in adjacent images through the thickness of a Sn film. The blue and gray whiskers have distinct orientations that differ by ∼77°.

distributions, grain and subgrain orientations, and to identify the local grain-boundary network.

We have begun experiments to characterize the local crystallographic structure within and near Sn whiskers formed from a thin Sn layer deposited on Cu. As illustrated in Fig. 9, it is possible to survey the thin-film region and determine the crystallographic structure of Sn whiskers and the local neighbor grains. These precision measurements of grain-boundary type also provide rare CSL measurements on a non-cubic material. The local grain-boundary network, the whisker orientation and the local strain state within the whisker and surrounding grains can all be characterized to test whisker growth theories.

4. Conclusion

The unprecedented characterization capabilities of three-dimensional polychromatic microdiffraction enable new scientific opportunities to explore mesoscale structure and dynamics. As illustrated above, polychromatic microdiffraction is particularly well suited to long-standing questions concerning three-dimensional and thin-film grain growth physics, and questions concerning deformation and the role of local environment and boundary conditions on elastic and plastic deformation.

In thin films, where spatial resolution along the incident beam is not essential, small volumes can be rapidly characterized with angular resolution less than 0.01°. The elastic deviatoric strain tensor elements can also be measured to

about one part in 10^4 in good single crystals. Both the uncertainty of the crystallographic orientation and uncertainty in the elastic strain tensor elements increase with the presence of significant dislocation density. Grains below 1 μm^3 are difficult to resolve, and for a low-Z sample only about five to ten grains can be indexed without the application of differential aperture microscopy. Thin-film volumes as small as $\sim$0.5 μm $\times$ 0.5 μm $\times$ 0.1 μm can be studied with good signal-to-noise if the volume is not too mosaic.

Characterization speed is limited primarily by the readout time of the CCD area detector; data-acquisition times are about 10–100 ms but CCD readout times take about 2–6 s. Therefore in thin films about 10 to 30 pixels of information can be collected each minute. With differential aperture microscopy, about an order of magnitude more measurements are required to resolve each volume element along the incident beam. As a result, differential aperture measurements take about 20–60 s per voxel.

Emerging X-ray optics and techniques will expand the range of materials that can be explored and the quantity and quality of information that can be recovered. New X-ray optics will provide spatial resolution below 100 nm with the hope of reaching $\sim$50 nm in 2005. Faster detectors and new differential aperture techniques are certain to improve data-acquisition times by orders of magnitude. For example, commercially available detectors can accelerate the data acquisition by a factor of at least 40 with no compromise to the data quality. More advanced collection strategies can similarly accelerate data collection by an order of magnitude, and measurements that currently require about 24 h of data collection (*e.g.* $\sim$5000 voxels) will be finished in four or five minutes. These advances will allow for real-time and *in situ* studies certain to advance our understanding of mesoscale structure and dynamics.

The authors wish to acknowledge the important contributions and support of Dr Jin-Seok Chung, Dr Nobumici Tamura and Dr Walter Lowe. Work was performed on beamlines 34-ID and 7-ID at the Advanced Photon Source. This research is supported by the US DOE, Basic Energy Sciences, Office of Science under contract DE-AC05-00OR22725 with UT-Battelle LLC. The UNICAT facility 34-ID at the Advanced Photon Source (APS) is supported by the US DOE under Award No. DEFG02-91ER45439 through the Frederick Seitz Materials Research Laboratory at the Universtiy of Illinois at Urbana-Champaign and by the Oak Ridge National Laboratory (US DOE contact DE-AC05-00OR22725 with UT-Battelle LLC). The APS and beamline 7-ID are supported by the US DOE, Basic Energy Sciences, Office of Science under contract No. W-31-109-ENG-38.

References

Arsenlis, A. & Park, D. M. (1999). *Acta. Mater.* **47**, 1597–1611.
Bollmann, W. (1982). *Crystal Lattices, Interfaces, Matrices: An Extension of Crystallography*. ISBN 2–88105-000-X.
Budai, J. D., Yang, W., Tamura, N., Chung, J.-S., Tischler, J. Z., Larson, B. C., Ice, G. E., Park C. & Norton, D. P. (2003). *Nature Mater.* **2**, 487–492.
Chevallier, P. & Dhez, P. (1997). *Accelerator Based Atomic Physics Techniques and Applications*, edited by S. M. Shafroth and J. Austin, pp. 309–348. New York: AIP Press.
Choi, W. J., Lee, T. Y., Tu, K. N., Tamura, N., Celestre, R. S., MacDowell, A. A., Bong, Y. Y. & Nguyen, L. (2003). *Acta Mater.* **51**, 6253–6261.
Chung, J. S. & Ice, G. E. (1999). *J. Appl. Phys.* **86**, 5249–5256.
Goudeau, P., Villain, P., Tamura, N. & Padmore, H. A. (2003). *Appl. Phys. Lett.* **83**, 51–53.
Humphreys, F. J. (2001). *J. Mater. Sci.* **36**, 3833–3854.
Ice, G. E., Chung, J. S., Lowe, W., Williams, E. & Edelman, J. (2000). *Rev. Sci. Instrum.* **71**, 2001–2006.
Ice, G. E., Chung, J. S., Tischler, J. Z., Lunt, A. & Assoufid, L. (2000). *Rev. Sci. Instrum.* **71**, 2635–2639.
Ice, G. E. & Larson, B. C. (2000). *Adv. Eng. Mater.* **2**, 643–646.
Langevelde, F. V., Tros, G. H. J., Bowen, D. K. & Vis, R. D. (1990). *Nucl. Instrum. Methods B*, **49**, 544–550.
Larson, B. C., Yang, W., Ice, G. E., Budai, J. D. & Tischler, J. Z. (2002). *Nature (London)*, **415**, 887–890.
Lee, B. Z. & Lee, D. N. (1998). *Acta Mater.* **46**, 3701.
Lee, T. Y., Choi, J., Chung, Y., Huang, J. Y., Lee J. M., Nam, S. H. & Youn, H. S. (2001). *Nuc. Instrum. Methods*, A**467**, 47–50.
Liu, C., Assoufid, L., Conley, R., Macrander, A. T., Ice, G. E. & Tischler, T. Z. (2003). *Opt. Eng.* **42** 12.
Liu, C., Conley, R., Assoufid, L., Macrander, A. T., Ice, G. E., Tischler, J. Z. & Zhang, K. (2003). *J. Vac. Sci. Technol. A*, **21**, 1579–1584.
Norton, D. P., Goyal, A., Budai, J. D., Christen, D., Kroeger, D., Specht, E. D., He, Q., Saffian, B., Paranthaman, M., Klabunde, C., Lee, D., Sales, B. & List, F. (1996). *Science*, **274**, 755–757.
Nye, J. F. (1953). *Acta Met.* **1**, 153.
Offerman, S. E., van Dijk, N. H., Sietsma, J., Grigull, S., Lauridsen, E. M., Margulies, L., Poulsen, H. F., Rekveldt, M. T. & van der Zwaag, S. (2002). *Science*, **298**, 1003–1005.
Palumbo, G. & Aust, K. T. (1992). *Materials Interfaces: Atomic Level Structure and Properties*, ch. 5, edited by D. Wolf and S. Yip London: Chapman and Hall.
Park, Y. H., Yeom, H. Y., Yoon, H. G. & Kim, K. W. (1997). *J. Appl. Cryst.* **30**, 456–460.
Poulsen, H. F. (2003). *Philos. Mag.* **83**, 2761–2778.
Poulsen, H. F., Nielsen, S. F., Lauridsen, E. M., Schmidt, S., Suter, R. M., Lienert, U., Margulies, L., Lorentzen, T. & Jensen, D. J. (2001). *J. Appl. Cryst.* **34**, 751–756.
Randle, V. (1993). *The Measurement of Grain Boundary Geometry*. Bristol: Institute of Physics.
Randle, V. & Davies, H. A. (2002). *Ultramicroscopy*, **90**, 153–162.
Ravelli, R. B. G., Hezemans, A. M. F., Krabbendam, H. & Kroon, J. (1996). *J. Appl. Cryst.* **29**, 270–278.
Rebonato, R., Ice, G. E., Habenschuss, A. & Bilello, J. C. (1989). *Philos. Mag. A*, **60**, 571–583.
Rogan, R. C., Tamura, N., Swift, G. A. & Üstündag, E. (2003). *Nature Mater.* **2**, 379–381.
Schwartz, A. J., Kumar, M. & Adams, B. L. (2000). *Electron Backscattering Diffraction in Materials Science*. New York: Kluwer/Plenum.
Sheremetyev, I. A., Turbal, A. V., Litvinov, Y. M. & Mikhailov, M. A. (1991). *Nucl. Instrum. Methods A*, **308**, 451–455.
Sparks, C. J. (1980). *Synchrotron Radiation Research*, edited by H. Winick and S. Doniach, pp. 459–512. New York: Plenum.
Tamura, N., MacDowell, A. A., Spolenqak, R., Valek, B. C., Bravman, J. C., Brown, W. L., Celestre, R. S., Padmore, H. A., Batterman, B. W. & Patel, J. R. (2003). *J. Synchrotron Rad.* **10**, 137–143.
Valek, B. C., Bravman, J. C., Tamura, N., MacDowell, A. A., Celestre, R. S., Padmore, H. A., Spolenak, R., Brown, W. L., Batterman, B. W. & Patel, J. R. (2002). *Appl. Phys. Lett.* **81**, 4168–4170.

Valek, B. C., Tamura, N., Spolenak, R., Caldwell, W. A., MacDowell, A. A., Celestre, R. S., Padmore, H. A., Bravman, J. C., Batterman, B. W., Nix, W. D. & Patel J. R. (2003). *J. Appl. Phys.* **94**, 3757–3761.
Watanabe, T. (1984). *Res. Mech.* **11**, 47–84.
Wenk, H. R., Heidelbach, F., Chateigner, D. & Zontone, F. (1997). *J. Synchrotron Rad.* **4**, 95–101.
Xu, S. L., Lai, B. & Viccaro, P. J. (1992). *APS Undulator and Wiggler Sources: Monte-Carlo Simulations*, ANL/APS/TB-1. Advanced Photon Source, IL, USA.
Yang, W. G., Larson, B. C., Ice, G. E., Tischler, J. Z., Budai, J. D., Chung, K. S. & Lowe, W. P. (2003). *Appl. Phys. Lett.* **82**, 3856–3858.